Applied Catalysis B: Environmental 164 (2015) 225–233

Contents lists available at ScienceDirect

Applied Catalysis B: Environmental

journal homepage: www.elsevier.com/locate/apcatb

Vanadium and alumina modified with groups I and II elements for CO_2 and coke reaction under fluid catalytic cracking process

Thiago Crispim da Silva[a,b,c], Joana Filipa Pinto[a,d], Fabiana M. Santos[a], Luciana T. dos Santos[e], Donato A.G. Aranda[e], Filipa Ribeiro[d], Nuno Batalha[a], Marcelo Maciel Pereira[a,*]

[a] Instituto de Química – Universidade Federal do Rio de Janeiro, Av. Athos da Silveira Ramos, Rio de Janeiro, RJ, Brazil
[b] Departamento de Química Inorgânica, Instituto Federal de educação, ciência e tecnologia do Rio de Janeiro, R. Lúcio Tavares, Nilópolis, RJ, Brazil
[c] Escola de Química – Universidade Federal do Rio de Janeiro, Av. Athos da Silveira Ramos, Rio de Janeiro, RJ, Brazil
[d] Institute for Biotechnology and Bioengineering (IBB), Centre for Biological and Chemical Engineering, Instituto Superior Técnico, Universidade de Lisboa, Av. Rovisco Pais, 1049-001 Lisboa, Portugal
[e] Agência Nacional de Petróleo, Av. Rio Branco, Rio de Janeiro, RJ, Brazil

ARTICLE INFO

Article history:
Received 1 July 2014
Received in revised form
10 September 2014
Accepted 13 September 2014
Available online 29 September 2014

Keywords:
CO_2
FCC
Coke
Regeneration
Alkaline metals

ABSTRACT

The fluid catalytic cracking process is responsible for about 30% of CO_2 emission in a petroleum refinery. The possibility to react CO_2 and coke (Reverse-Boudouard reaction – RB) during the spent catalyst regeneration in the presence of CO_2 and O_2 atmosphere, instead of air, can simultaneously mitigate CO_2 emission and produce CO for sequential uses. This goal was achieved by using an alumina modified by vanadium and potassium. Catalysts composed of alumina modified by Li, Na, K, Mg and Ca were investigated. The modified alumina catalysts were active for RB reaction in the following order, K > Mg, Li > Ca, Na > pristine alumina. Alumina modified by vanadium and potassium was also studied and revealed itself a remarkably active catalyst under O_2 atmosphere, as well as for RB reaction. For instance, at 720 °C 50% of CO_2 was converted to CO, this value increases to 90% at 800 °C. Finally, insights into RB reaction were provided performing this reaction in the presence of $^{13}CO_2$.

1. Introduction

Around 10^{20} J year^{-1} are required for all Human being activities in world [1]. Such high amount of energy is provided mainly by burning fossil fuels, resulting in a large amount CO_2 emissions expressed as roughly 8 GTon of carbon/year [2]. This carbon dioxide spreads through the planet, part of it being absorbed through several natural mechanisms [3] while the remaining portion is accumulated in the atmosphere. Despite several uncertainties for quantification, carbon absorption by Earth itself represents about 50% of all CO_2 emitted. In a huge contrast less than 0.1% of CO_2 produced by anthropogenic sources has been recycled or mitigated [4]. The possibility of using CO_2 as a reactant in the refinery structure could largely contribute to decreasing greenhouse emission. In this sense, the Fluid Catalytic Cracking process (FCC) is a key to reach such goal. FCC is the most important conversion process in several refineries, being installed for converting vacuum gasoil or atmospheric residue into several products, such as gasoline and light cycle oil [5]. Coke formation is a consequence of hydrocarbon cracking reactions on solid acid catalysts [6]. Moreover, the coke amount in the spent catalyst is related to the processed feed, *i.e.* lower quality feeds result in greater coke formation in the spent catalyst.

The spent catalyst regeneration in rich CO_2 atmosphere, as presented in Fig. 1, simultaneously combines CO_2 capture with CO production for sequential uses, *i.e.* hydrogen [7], methanol [8], dimethylether [9,10] and hydrocarbons [11,12] production. However, so far this approach has not been achieved because O_2 reactivity as oxidant is several orders of magnitude higher than that for CO_2 [13,14].

The CO_2 and coke reaction is known as the Reverse-Boudouard reaction (RB). The global RB reaction ($C + CO_2 \rightarrow 2CO$) [15,16] is largely endothermic (160–200 kJ mol^{-1}) [17,18], however the partial reaction (Scheme 1a) is slightly exothermic on both graphite [18] and model compounds [15]. On the other hand, on carbon surfaces promoted with potassium salts the enthalpy for this partial reaction varies from slightly exothermic to moderately

* Corresponding author. Tel.: +55 21 39387240; fax: +55 21 39387559.
E-mail addresses: maciel@iq.ufrj.br, marcelo.maciel.pereira@gmail.com (M.M. Pereira).

http://dx.doi.org/10.1016/j.apcatb.2014.09.028
0926-3373/

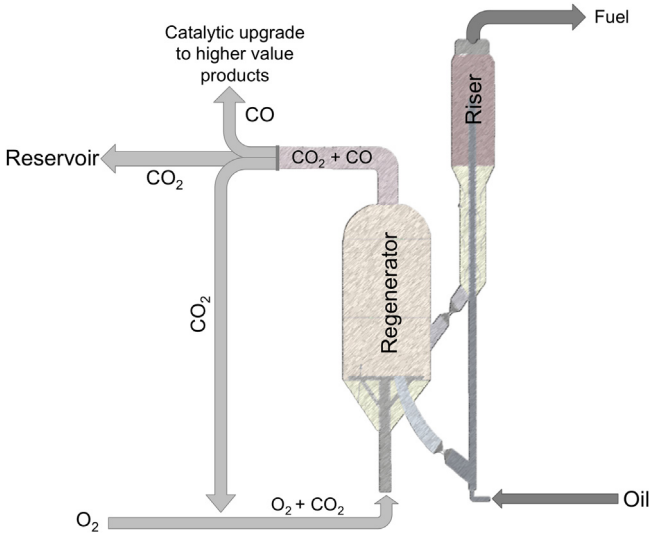

Fig. 1. Work proposal: CO_2 mitigation by its use as a chemical impute into the refinery structure. Oxygen is obtained in an air separation unit and mixed with CO_2 for regeneration of spent catalyst in FCC unit. High concentrated flows of CO_2 and CO are produced for sequential uses.

Scheme 1-a: CO_2 + Coke → CO + Coke-O

Scheme 1-b: Coke-O → CO/CO_2

Scheme 1-c: Coke-O + O_2 → CO/CO_2

Scheme 1-d: CO + Coke → (CO)-Coke

Scheme 1. Reaction steps involved in FCC catalyst regeneration in CO_2/O_2 atmosphere.

endothermic [19] according to oxygenation degree of the coke, *i.e.* the reaction is more endothermic over more oxygenated coke. On the other hand, the second CO formation (Scheme 1b) is largely endothermic, since it involves decomposition of oxidized groups on coke/graphite surface [18]. Consequently, a technological approach for performing spent catalyst regeneration in the presence of CO_2 should involve the partial reaction of coke with CO_2 (Scheme 1a) and sequentially/simultaneously the residual coke should be burned with oxygen [20], as represented in Scheme 1c [21,22]. Finally CO could form more stable species on coke, Scheme 1d.

There is a high amount of work focused on gas/solid reaction between CO_2 and coke promoted by alkali salts [19,23]. Carbonates of group I and II are easily formed [24–27]. On the other hand, oxygen scrambling was demonstrated between labeled oxygen CO_2 and MgO [24]. During dry catalytic reforming there are many proposals involving the formation of oxide-bicarbonate species [28–31]. The hydrogen formed by hydrocarbon reactions on metal particles undergoes migration to the interface of the metal–particle and support [29,32–34], which combined with oxygen atoms (provided by CO_2) leads to water formation.

Vanadium is largely used as a catalyst for oxidative/dehydrogenation reactions in the presence of O_2 [35,36]. Vanadium is also a common contaminant in most FCC feeds [37] and its mobility among the constituents of the catalyst was largely explored [38]. This peculiarity can be used in favor of RB reaction since the catalyst could be formed *in situ* during the spent catalyst regeneration. Moreover, vanadium-potassium alumina catalysts were proven to remarkably enhance SO_x mitigation [39].

In contrast to carbon/coke gasification (in CO_2) where alkali promoter was added on the carbon, the FCC requires a proper catalyst where the promoters are introduced. Therefore, coke will be deposited on the catalyst. This situation is rather different when compared to coke gasification promoted by alkali metal in the presence of CO_2 or H_2O. Following this idea it was recently shown by our group in a short publication [40] that when alumina was modified by both potassium and vanadium a synergetic effect between them largely increased RB reaction. Apparent activation energy for pristine alumina, potassium alumina and potassium and vanadium on alumina were 349, 249 and 192 kJ mol^{-1}, respectively. Moreover, it was shown that at 700 °C when RB reaction is carried out in the presence of O_2, CO_2 and O_2 reacted with coke in molar proportion of 1 to 1.6 respectively during 5 min of time on stream. Therefore it was suggested that thermal balance could be attained in the FCC process.

Herein, we explore the RB reaction over alumina modified by lithium, sodium, potassium, magnesium and calcium (spent FCC catalyst was included as reference). In addition, considering previous results observed on vanadium–potassium–alumina catalysts, the RB reaction was investigated in a broad range of temperature and a proper catalyst characterization was done. Finally, $^{13}CO_2$ was used in order to provide insights into the reaction pathway.

2. Experimental

2.1. Catalyst preparation

2.1.1. Alumina modified with groups I and II elements

The modified alumina catalysts were synthesized by mechanically mixing bohemite, gently provided by Petrobras, with chloride salts of lithium, sodium, potassium, calcium and magnesium. The amount of group I and II chloride salts in the mixture was determined to obtain a 5 wt.% final mixture in alumina. The samples were homogenized, placed in porcelain capsules and thermally treated under air atmosphere. The final modified alumina supports were then obtained by thermal treatment of the bohemite/chloride salt mechanical mixture at 850 °C for 10 h under dry air atmosphere. It is important to notice that 850 °C is sufficient to reach the melting temperature of all chloride precursors. The catalysts were named as Li/Al_2O_3, Na/Al_2O_3, K/Al_2O_3, Ca/Al_2O_3 and Mg/Al_2O_3. Additionally, a non-modified alumina sample (Al_2O_3) was prepared to use as comparison and an equilibrium FCC catalyst was used as reference [41].

2.1.2. Vanadium addition

Vanadium supported catalysts were prepared by incipient wetness impregnation using an aqueous solution of vanadyl acetylacetonate (vanadium(IV)-oxyacetylacetonate, VAA, Aldrich, 95 wt.%). The samples were placed in contact with the VAA solution in a rotary evaporator at 60 °C under reduced pressure for 2 h. The remaining solids were dried at 120 °C over night and thermal treated at 600 °C for 3 h under dried air atmosphere. The catalyst preparation was performed to obtain a final loading of 1 wt.% of vanadium. Only K/Al_2O_3 and Al_2O_3 were modified by vanadium addition. Final catalysts were named $V\text{-}K/Al_2O_3$ and V/Al_2O_3.

2.1.3. Catalyst coking

The spent catalysts were obtained by a catalytic cracking test in an ACE-Advanced Catalytic Evaluation at (CENPES/Petrobras). It was used 1.8 g of a vacuum gas oil feed and 9 g of catalyst in a fixed bed reactor, cracking reaction was carried out at 535 °C, during 90 s, then the spent catalyst was purged at the same temperature during 6 min in nitrogen atmosphere for removing light hydrocarbon adsorption and stabilizing the formed coke.

2.2. Catalyst characterization

The textural characterization was carried out in a Micromeritics ASAP 2010. Initially, the catalysts were pretreated at 200 °C under

vacuum during 2 h, then the isotherms of adsorption of nitrogen at 77 K were performed and specific surface area was determined though the BET method.

The groups I and II elements, as well as the vanadium global compositions were determined by X-ray fluorescence analysis using a Rigaku RIX3100 fluorescence spectrophotometer. In the particular case of Al_2O_3, K/Al_2O_3, V/Al_2O_3 and $K\text{-}V/Al_2O_3$ XPS analyses were performed to obtain the surface composition of the catalysts. The XPS analyses were performed on an Escalab 250 XIThermo Scientific equipment, with an AlKα monochromatic radiation of 1486.6 eV and at pressure of 1×10^{-9} mbar.

The X-ray powder diffraction (XRD) patterns were obtained using a Rigaku X-ray diffractometer with nickel-filtered CuKα1 radiation source (λ = 0.15406 nm) and graphite monochromator. The XRD profiles were collected in the 2θ angle region between 5° and 80°, at a step width of 0.05°, counting 1 s between each step.

Solid-state ^{13}C NMR spectra were recorded on a Bruker Avance III 400 (9.4 tesla) spectrometer, operating at 100.6 MHz respectively. The spinning rate was 15 KHz and 4 mm probe was used. Experimental parameters were the following: high power proton decoupled ^{13}C (HPDEC), repetition time $D1$ of 60 s and pulse width $(\pi/2) - 4$ μs.

CO_2 adsorption was carried out in thermogravimetric analysis (Netzsch STA449 F1 Jupiter) for Al_2O_3, K/Al_2O_3, V/Al_2O_3 and $V\text{-}K/Al_2O_3$. Previously to CO_2 adsorption the catalyst was dried at 500 °C for 1 h under helium atmosphere. At 50 °C the catalyst was exposed to a flow of 10%CO_2 in helium during 60 min. The catalyst weight gain was related to CO_2 adsorption. Then, the temperature was increased from 50 °C to 700 °C. At higher temperatures no CO_2 adsorption was observed.

The amount of coke in the spent catalysts was determined through thermogravimetric analysis (Netzsch TG-IRIS). The samples were heated, under helium atmosphere, from 35 to 150 °C at a rate of 10 °C min^{-1} and remained at 150 °C for 30 min, after which the temperature was raised to 800 °C at 10 °C min^{-1}. Once arrived at 800 °C the atmosphere was switched to 5% O_2 in He while the temperature increased until 1000 °C at 10 °C min^{-1}. The amount of coke for each sample was determined by the weight loss after 535 °C (reaction temperature).

2.3. Spent catalyst regeneration

The spent catalysts were submitted to two experimental procedures as described below. In all cases the formed gases were monitored by on line Mass Spectrometer MKS (model PPT430).

In the first experimental procedure the mass spectra were collected continuously during the sample heating from 25 °C to 1000 °C at a heating rate of 10 °C min^{-1} under flow of 60 mL min^{-1} in three different atmospheres (pure He, 5% O_2/He, and 10% CO_2/He).

In the second experimental procedure the spent catalysts were heated from 25 °C to the reaction temperatures (680, 760, 800, 860, 900 and 940 °C) at a heating rate of 10 °C min^{-1} under a He flow of 60 mL min^{-1} and kept under these conditions until the mass spectra profiles stabilized. Then 0.472 mmol of $^{13}CO_2$ was introduced in helium flow. $^{13}CO_2$ was produced by means of $Na_2{}^{13}CO_3$ decomposition as described elsewhere [41].

3. Results

3.1. Catalyst characterization

Textural properties of all used catalysts are presented in Table 1 showing that in all cases the specific surface area of alumina decreases upon modification with alkaline metals.

Table 1
Catalysts, textural properties, coke amount and percentage of coke burn for both O_2/He and CO_2/He atmosphere.

Catalysts	Metal (wt.%)	Coke (wt.%)	S_{BET} ($m^2\ g^{-1}$)	Coke (wt.% m^{-2})
Al_2O_3	–	2.9	241	0.012
K/Al_2O_3	5.0	1.4	144	0.010
Na/Al_2O_3	1.7	0.9	95	0.009
Li/Al_2O_3	3.6	1.1	96	0.011
Ca/Al_2O_3	4.8	0.9	78	0.011
Mg/Al_2O_3	3.6	1.7	104	0.017
$V\text{-}K/Al_2O_3$	1.0 (V), 5.0 (K)	3.4	147	0.023
V/Al_2O_3	1.0	3.9	101	0.039
E-Cat FCC	–	1.27	115	0.011

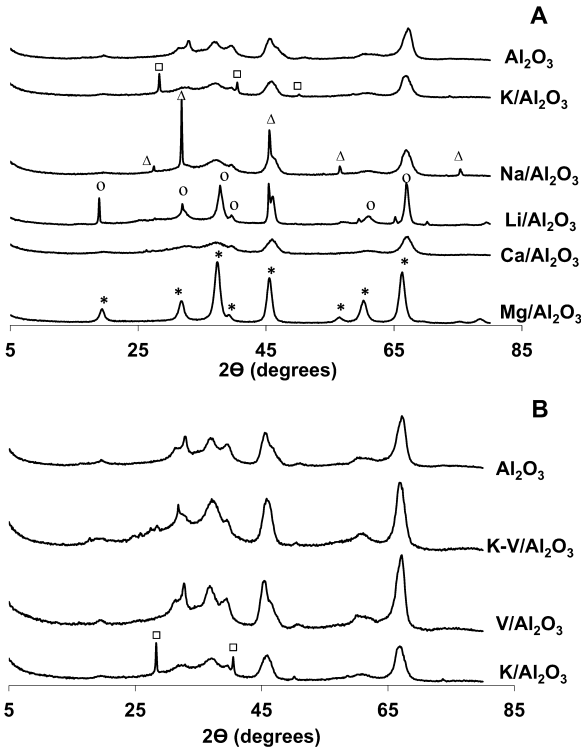

Fig. 2. X-ray diffraction patterns. (A) Alumina modified with groups I and II elements. (B) Alumina modified with vanadium and potassium. (□) KCl; (△) NaCl; (◯) $LiAlO_2$; (*) $MgAl_2O_4$.

XRD diffraction patterns of all used catalysts are shown in Fig. 2. A clearly shows that depending on the chloride salt used to modify alumina different phases can be observed. In the particular case of K/Al_2O_3 and Na/Al_2O_3 the respective NaCl and KCl salts were still observed. On the other hand, the Mg/Al_2O_3 catalyst was composed of $MgAl_2O_4$ spinel phase. The Li/Al_2O_3 XRD diffractogram showed a mixture of alumina and lithium aluminum oxide, while the ones of Ca/Al_2O_3 did not present a major variation when compared to pristine alumina. On the other hand, by adding vanadium to K/Al_2O_3 caused the characteristic KCl salt diffraction peaks disappearance (Fig. 2b), this was already observed for all group I and II prepared using metal chloride [39].

XPS was carried out for Al_2O_3, V/Al_2O_3, K/Al_2O_3 and $V\text{-}K/Al_2O_3$ catalysts, and the results are shown in supplementary information Table S1. V/K ratio (measured by XPS) in $V\text{-}K/Al_2O_3$ catalyst was 0.13 while the same ratio based on catalyst composition was 0.18. On the other hand, $V\text{-}K/Al_2O_3$ had a V/Al (XPS) ratio of 0.012, which was 50% lower than that of V/Al_2O_3. These results suggest that vanadium should form some type of compound, probably with potassium. This high V and K interaction was previously observed for a catalyst containing 5 wt.% of vanadium and 5.8 wt.% K on

alumina that all potassium was covered with vanadium [39]. Indeed, vanadium is well known to interact with alkaline metal oxides forming either VO_3-MOx or V_2O_7-MOx species on the metal oxide surface [42–44]. The type of compound formed depends both on the alkaline metal oxide and the vanadium loading used.

A comprehensive CO_2 adsorption/desorption study was carried out to better study the impact of vanadium addition to potassium catalyst on CO_2 interaction. According to Ref. [45], CO_2 adsorption disclosed several peculiarities of the alumina surface. Three distinct regions were observed during isothermic adsorption: up to 15 μmol CO_2 g^{-1}, monodentate carbonate species with heat adsorption from 130 to 105 kJ mol^{-1}; bi-carbonates from 15 to 130 μmol CO_2 g^{-1}, having heat of adsorption from 105 to 50 kJ mol^{-1} (that is slowly converted into carbonate); and, weak adsorbed species above 130 μmol CO_2 g^{-1}. CO_2 adsorption at 50 °C was carried out for Al_2O_3, V/Al_2O_3, K/Al_2O_3 and $V\text{-}K/Al_2O_3$ catalysts, the CO_2 adsorption weight gains were 0.4, 0.3, 3.1 and 1.9 wt.%, respectively, *i.e.* 68, 90, 704 and 431 μmol of CO_2 per gram of catalyst. The huge difference between Al_2O_3, V/Al_2O_3 and K/Al_2O_3 weight increase was due to the high capacity of potassium to adsorb CO_2. The $V\text{-}K/Al_2O_3$ sample showed 40% less CO_2 adsorption capacity than its parent K/Al_2O_3, despite potassium concentration on the surface (measure by XPS) being quite similar, *i.e.* around 2.5% and yet, both catalysts showed the same BET surface area. These results suggest once again that vanadium and potassium are forming some type of compound in $V\text{-}K/Al_2O_3$ catalyst. Indeed, vanadium is well known to interact with the alkaline metal oxides surface forming VO_3-MOx or V_2O_7-MOx species [42–44], impeding the CO_2 adsorption as carbonate. Still, it is important to notice that CO_2 adsorption at temperatures higher than 500 °C was not observed by TG measurements.

3.2. Coke characterization in spent catalysts

Coke amount in spent catalysts (see Table 1) was higher on alumina, however the values of coke per area of catalyst (coke wt.% m^{-2}) were similar and around 0.01 for most (in all) spent catalysts, excluding Mg/Al_2O_3, V/Al_2O_3 and $V\text{-}K/Al_2O_3$ catalysts. Coke nature was investigated by thermo desorption in helium flow as well as by ^{13}C NMR. The carbon–oxygen functionality in coke was correlated to both CO and CO_2 profiles in helium atmosphere [46] (profiles for Al_2O_3 and K/Al_2O_3 are shown in Figs. S1 and S2, respectively for CO and CO_2 formation). CO profiles were similar for all catalysts with CO being formed from 650 °C to 900 °C, particularly in one main peak around 815–850 °C. The CO formed in this temperature range was related to highly stable compounds, for instance, CO release around 850 °C and 750 °C is related to quinone and carboxylic type compounds respectively [46]. Pristine alumina showed a very similar CO profile, but there is a slight shoulder dislocated to higher temperatures, which could be related to the higher amounts of carbonyl or hetero cycles compounds in this spent catalyst, as observed in the ^{13}C NMR analysis. CO_2 profiles were also similar in all spent catalysts. CO_2 was formed from 500 °C to 800 °C as presented in Fig. S2. These regions confirmed those coke-oxidized species based on CO profiles and yet, the released CO_2 was slight dislocated to higher temperatures for pristine alumina, as observed for CO formation. Moreover, a peak at 240 °C was observed only in K/Al_2O_3 catalyst, this CO_2 formation could be related to adsorption on potassium sites.

Coke on spent Al_2O_3, K/Al_2O_3 and $V\text{-}K/AL_2O_3$ catalysts was similar and mainly composed of poly-aromatic carbons (Fig. S3). Tertiary and quaternary aromatic carbons in the range of 160 to 90 ppm were the main representative carbon atoms (roughly 80%). Carbonyl compounds and aliphatic carbons ascribed to ppm in the range of 200–160 and 50–0, respectively, were slightly lower in the spent K/Al_2O_3 when compared with spent Al_2O_3 and $V\text{-}K/Al_2O_3$.

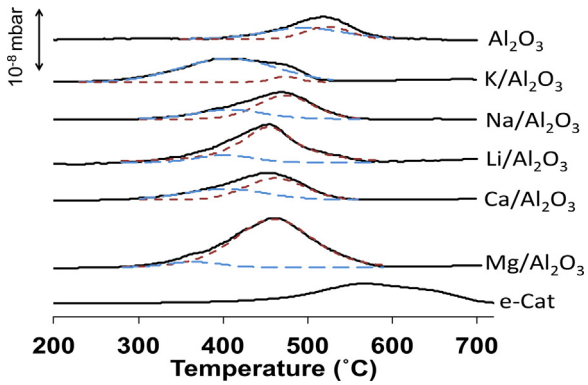

Fig. 3. Spent alumina modified with groups I and II elements regeneration profile in O_2 (5%)/He atmosphere (TPO). CO profiles deconvolution presented in color with peak center temperatures described in Table 3.

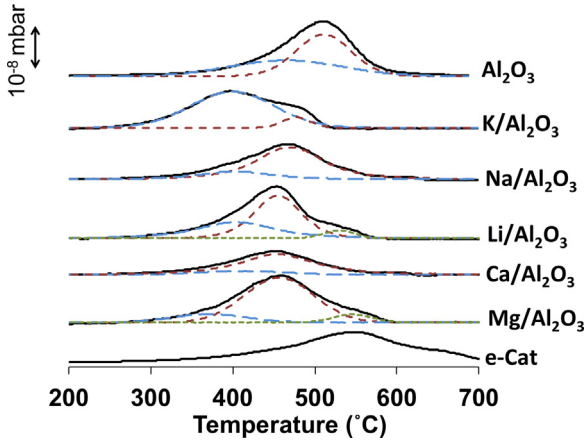

Fig. 4. Spent alumina modified with groups I and II elements regeneration profile in O_2 (5%)/He atmosphere (TPO). CO_2 profiles deconvolution presented in color with peak center temperatures described in Table 3.

Coke in the spent FCC catalyst is also mainly composed by poly-aromatic as presented elsewhere [41].

3.3. Spent catalyst regeneration promoted by alumina modified by groups I and II elements

3.3.1. Regeneration in O_2/He atmosphere

Regeneration profiles of the spent catalysts in O_2/He atmosphere (TPO experiment) are shown in Figs. 3 and 4 and Table 2. Coke conversion was complete in all catalyst. CO profiles of spent Al_2O_3, K/Al_2O_3, Na/Al_2O_3, Li/Al_2O_3, Ca/Al_2O_3, Mg/Al_2O_3 and e-cat are presented in Fig. 3. Spent FCC catalyst (e-cat) showed that coke burned at similar temperatures to those reported in Refs. [21,41], even at higher temperatures than the latter catalysts. These differences are caused in part by the coke type of the e-cat, which has a higher composition of poly-aromatics quaternary carbons [47]. In all spent catalysts, the CO profile was composed of different CO peaks. On Al_2O_3, where no alkaline metal was present, the CO formation occurred at higher temperatures with the first peak occurring at 496 °C and the second at 523 °C. On the other hand, the remaining spent alumina catalysts presented two CO peaks: the first occurring between 400 and 410 °C and the second 450–470 °C. Mg/Al_2O_3 catalyst also presented a CO formation? Peak around 460 °C, however a small CO formation was observed around 365 °C. Despite the similarity between the CO formation temperatures among the spent catalysts, the proportions of the two regions were quite different. For instance, K/Al_2O_3 first and second peak

Table 2
CO and CO_2 formation peak center after deconvolution of the profiles obtained during the group I and II doped spent catalysts regeneration in O_2 (5%) in helium atmosphere. CO and CO_2 profiles shown in Figs. 3 and 4, respectively.

	CO peak (°C)		CO_2 peak (°C)					CO/CO_2
	1st	2nd	1st/2nd	1st	2nd	3rd	1st/(2nd + 3rd)	
Al_2O_3	496	523	–	–	465	510	–	0.07
K/Al_2O_3	406	473	14.6	399	477	–	10.3	0.19
Na/Al_2O_3	408	473	0.5	402	470	–	0.3	0.21
Li/Al_2O_3	402	453	0.2	403	454	529	0.0	0.26
Ca/Al_2O_3	402	461	0.9	410	454	–	0.0	0.39
Mg/Al_2O_3	365	460	0.01	371	456	545	0.2	0.40

ratio (400–410 °C and 450–470 °C, respectively) was 14.6 whereas for Li/Al_2O_3 it was 0.2. Indeed, it can be observed that there are huge differences among these values.

CO_2 formation profiles are shown in Fig. 4. The temperature ranges observed were quite similar to the ones observed for CO. Just like for CO, most spent catalysts evidenced two distinct CO_2 formation peaks: the first around 400–410 °C and the second around 450–470 °C. On Li/Al_2O_3 and Mg/Al_2O_3, however, a third smaller peak was verified respectively at 529 °C and 545 °C. As before, the proportion between the first and second peaks changed with the alkaline metal in use: K/Al_2O_3 >>Na/Al_2O_3, Mg/Al_2O_3 > Ca/Al_2O_3, Li/Al_2O_3. The observed tendency is not the same as the one observed for CO. It is important to notice that the CO_2 amount released during the catalyst burning in O_2/He atmosphere was higher than CO for all catalysts (Table 2). Still, all modified alumina produced more CO than pristine alumina, in particular when modified with group II elements.

The addition of group I and group II elements to alumina displaced the coke burning to lower temperatures. If considering that coke deposited over these catalysts can be located in two main regions: the first, over an area richer in alkaline metals and the other one on alumina it would be expected for the CO and CO_2 profiles to reflect, at least in part, the pristine alumina profile. Nonetheless, this was not the case. Therefore, even if the coke is not in the vicinity of alkaline metals it still burns at lower temperatures than over pristine alumina, implying that oxygen mobility might be involved in the mechanism. Indeed, Zhang et al. demonstrated that oxygen spillover was involved in the potassium supported catalysts during soft catalytic combustion [48]. The effect of alkaline and alkaline earth metals for promoting combustion in the presence of O_2 has been recently reported [49] as well as for promoting petroleum coke steam gasification [50]. It was proposed in the latter that peroxide/hydro-peroxide species on potassium are related to the high activity for polyaromatics compounds decomposition [50].

3.3.2. *Spent catalyst regeneration in CO_2/He atmosphere (Reverse-Boudouard reaction)*

The CO formation profiles resulting from the spent catalysts regeneration in CO_2/He atmosphere are shown in Fig. 5. All the catalyst showed complete coke conversion with the exception of Al_2O_3 and e-cat where coke conversion was 40%. Al_2O_3 and e-cat catalyst showed a single and large CO formation peak around 920 °C and 940 °C, respectively, and in both cases, when the temperature reached 1000 °C, CO was still being formed. On the other hand, on all modified alumina catalysts the CO formation occurred at lower temperatures when compared with Al_2O_3. All modified alumina samples, with the exception of K/Al_2O_3, presented quite similar CO profiles composed by three main CO formation peaks (not shown in Fig. 5): the first around 780–800 °C; the second at 850 °C; and the third at 900–950 °C. K/Al_2O_3 was able to activate the CO_2 reaction with coke at much lower temperatures. Like the other modified alumina, three main CO formation peaks composed the K/Al_2O_3 profile, however these were at 700 °C, 760 °C and 810 °C. It is important to notice that in all catalysts, with the exception of Al_2O_3 and e-cat the coke was completely consumed during the reaction.

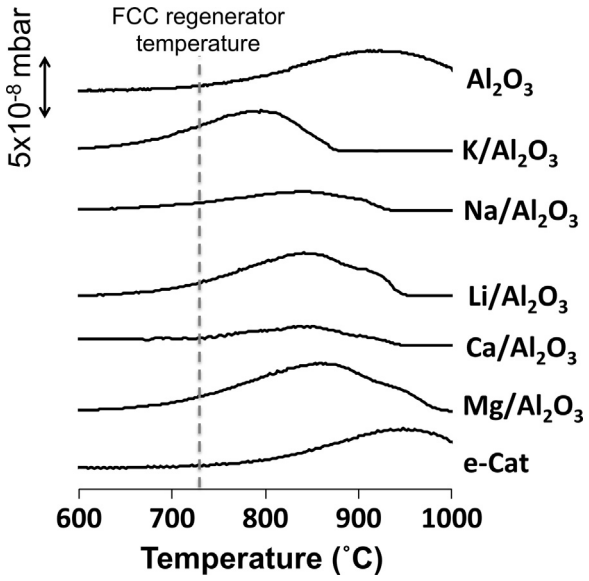

Fig. 5. CO formation profile of spent alumina modified with groups I and II elements in CO_2 (10%)/He atmosphere.

Among all the catalysts, K/Al_2O_3 was the one able to promote the RB reaction at lower temperatures, thus making the potassium the more suitable alkaline metal catalyst for this reaction. Moreover, the typical FCC regenerator temperature is around 720 °C. Temperatures up to 760 °C have also been reported [51]. Therefore, the temperature range on what the RB reaction occurs in this catalyst is still slightly higher than that required for it to be used in the FCC process.

3.4. *Spent catalyst regeneration promoted by alumina modified by both vanadium and potassium*

In a previous communication it was shown by our group that alumina modified by both potassium and vanadium was able to promote coke oxidation by CO_2 in the presence of O_2 [40]. Nevertheless, several facts still remain unclear about the potential of this type of catalyst for promoting the RB reaction itself.

3.4.1. *Regeneration in O_2/He atmosphere*

The vanadium addition to the K/Al_2O_3 catalyst caused a great change in TPO profiles temperatures, as presented in Figs. 6 and 7 (peak center temperatures shown in Table 3). Like the previously studied catalysts, two different peaks composed CO profiles: in V-K/Al_2O_3 and V/Al_2O_3 catalysts (Fig. 6). V/Al_2O_3 behavior was slightly different of that of alkaline metal catalysts, with the first CO release peak appearing at a lower temperature, 380 °C, and the

Table 3
CO and CO_2 formation peak center after deconvolution of the profiles obtained during the Al_2O_3, K/Al_2O_3, V/Al_2O_3 and $V\text{-}K/Al_2O_3$ spent catalyst regeneration in O_2 (5%) in Helium atmosphere. CO and CO_2 profiles shown in Figs. 3 and 4, respectively.

	CO peak (°C)		CO_2 peak (°C)					CO/CO_2
	1st	2nd	1st/2nd	1st	2nd	3rd	1st/(2nd + 3rd)	
Al_2O_3	496	523	–	–	465	510	–	0.07
$V\text{-}K/Al_2O_3$	355	395	1.5	282	333	–	0.39	0.08
V/Al_2O_3	380	464	1.3	373	461	–	0.39	0.35
K/Al_2O_3	406	473	14.6	399	477	–	10.3	0.19

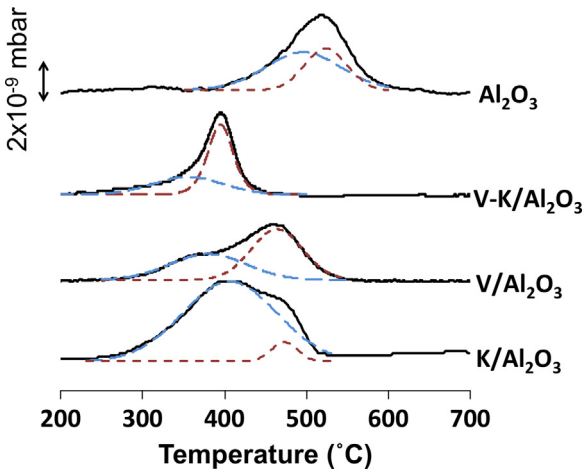

Fig. 6. Al_2O_3, K/Al_2O_3, V/Al_2O_3 and $V\text{-}K/Al_2O_3$ regeneration profile in O_2 (5%)/He atmosphere (TPO). CO profiles deconvolution presented in color with peak center temperatures in Table 4.

second at the usual temperature of 460 °C. The effect on temperature was enhanced in the $V\text{-}K/Al_2O_3$ catalyst, which showed CO peaks temperatures remarkably displaced to lower temperatures, *i.e.* 355 °C and 395 °C.

The V/Al_2O_3 CO_2 profile (Fig. 7) was in the same temperatures range to that observed to CO. Similarly, this was observed to all the remaining catalysts excluding the $V\text{-}K/Al_2O_3$. The later showed that CO_2 formation occurred at much lower temperatures than CO. In fact, the first CO formation peak (355 °C) occurred after the second CO_2 peak (333 °C). This phenomenon is quite surprising and clearly suggests that CO and CO_2 followed a very different reaction pathway over $V\text{-}K/Al_2O_3$ catalyst.

As can be easily seen in Figs. 6 and 7, the CO_2 amount formed with or on? All catalyst was much higher than the amount of CO. Still, $V\text{-}K/Al_2O_3$ formed 12 times more CO_2, while the V/Al_2O_3 and

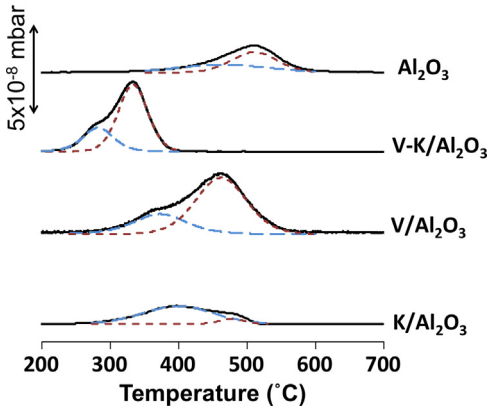

Fig. 7. Al_2O_3, K/Al_2O_3, V/Al_2O_3 and $V\text{-}K/Al_2O_3$ regeneration profile in O_2 (5%)/He atmosphere (TPO). CO_2 profiles deconvolution presented in color with peak center temperatures in Table 4.

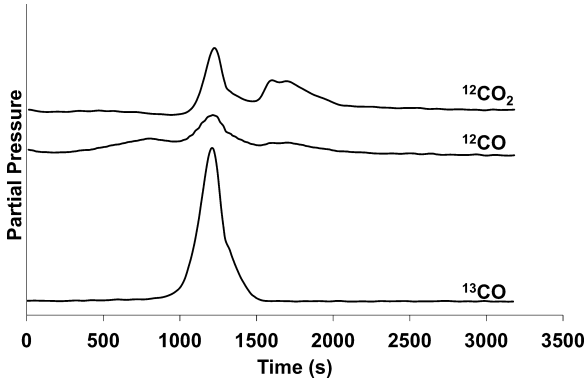

Fig. 8. Regeneration of spent K/Al_2O_3 catalyst in $^{13}CO_2$/He at 800 °C.

K/Al_2O_3 produced 2.5 and 5 times more CO_2, respectively. The higher CO_2 production at lower temperatures clearly indicates that $V\text{-}K/Al_2O_3$ is a powerful oxidation catalyst.

3.4.2. *Spent catalyst regeneration in CO_2/He atmosphere (Reverse-Boudouard reaction)*

Reverse-Boudouard reaction was studied through two different types of catalytic test: 1 – continuous heating in CO_2 (10%)/He atmosphere; 2 – reaction in the presence of a pulse that injects 0.472 mmol of $^{13}CO_2$ in 30 mL min^{-1} under He flow during about 17 min.

Regeneration of spent Al_2O_3, K/Al_2O_3, V/Al_2O_3, $V\text{-}K/Al_2O_3$catalysts in 10% CO_2/He atmosphere previously reported [40] are shown in Fig. S4 (e-cat FCC was introduced in this figure). RB reaction was remarkably improved in the latter catalyst, therefore, a synergy between vanadium and potassium has been proposed.

The experiments using pulses of $^{13}CO_2$ were carried out in a broad range of temperatures. A typical profile is shown in Fig. 8. The reaction between $^{13}CO_2$ and the spent catalysts produced a ^{13}CO in one main peak accompanied by a smaller shoulder. Almost simultaneously to ^{13}CO a broad peak, ^{12}CO and $^{12}CO_2$ were formed (that could be split probably in two or more peaks). Successively, both Al_2O_3 and K/Al_2O_3 ^{12}CO and $^{12}CO_2$ showed a sequential peak. All profiles are presented in supplementary information Figs. S5–S7. By these profiles, it was clear that both ^{12}CO and $^{12}CO_2$ production were a consequence of the complex reaction pathway. However, it is important to point out that the sequential ^{12}CO and $^{12}CO_2$ formation observed on Al_2O_3 and K/Al_2O_3 was largely affected by reaction temperature. The higher the reaction temperature the faster these sequential species were formed. Yet, at higher temperatures the second peak was formed just after the first one in a broad main peak, this point will be further evaluated in Section 4. It is important to notice that the second ^{12}CO and $^{12}CO_2$ release peaks were not observed on $V\text{-}K/Al_2O_3$, indicating that the reaction pathway on this catalyst must be somewhat different of that in the remaining catalysts.

Semi-quantitative results of RB conversion were estimated by integrating the total area of each compound using the following

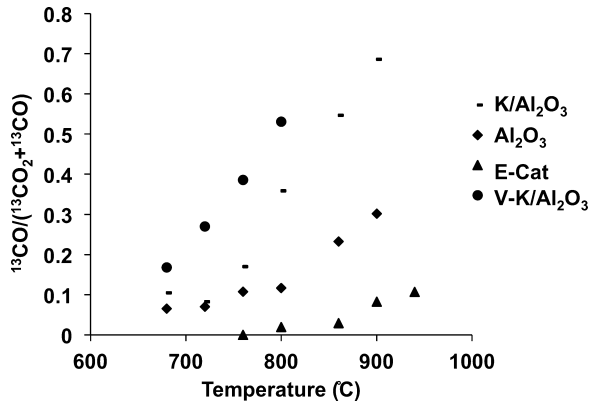

Fig. 9. CO_2 conversion into ^{13}CO (expressed by $^{13}CO/(^{13}CO_2 + ^{13}CO)$ of spent Al_2O_3, K/Al_2O_3 and FCC catalysts under $^{13}CO_2$/He from 680 °C to 900 °C. Values were correct by $^{13}CO_2$ fragmentation (CO_2 itself undergoes fragmentation producing 7% of CO, therefore the amount of CO_2 (not reacted) in each experiment were multiplied by 0.07, the CO amount was correct by this value).

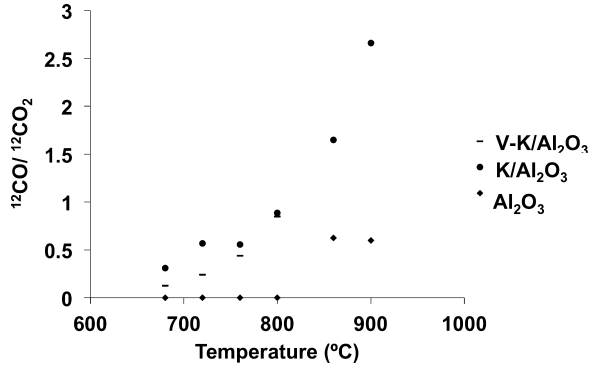

Fig. 10. $^{12}CO/^{12}CO_2$ ratio under $^{13}CO_2$/He of spent Al_2O_3, K/Al_2O_3 and $V\text{-}K/Al_2O_3$ from 680 °C to 900 °C.

equation: area of ^{13}CO/(area of $^{13}CO_2$ + area of ^{13}CO); ^{13}CO amount was correct by $^{13}CO_2$ fragmentation typical of the mass spectrum analyzer. The conversion results are present as a function of temperature (Fig. 9). Spent FCC catalyst (e-cat) was the least active catalyst for the RB reaction, only being able to transform a small portion of $^{13}CO_2$ into ^{13}CO at 800 °C. Pristine alumina also showed low RB reaction activity. Spent K/Al_2O_3 catalyst showed conversion rather superior to pristine alumina in all temperature range. However, spent $V\text{-}K/Al_2O_3$ was by far the most active catalyst for the RB reaction. Coke consumption, based on the amount of $^{13}CO_2$ consumed, is presented in Table 4 for K/Al_2O_3 and $V\text{-}K/Al_2O_3$ catalysts. The latter showed at 720 °C and 800 °C a $^{13}CO_2$ conversion of 50% and 90%, respectively. It is important to notice that a large amount of CO (both ^{12}CO and ^{13}CO) is formed. For instance, at 800 °C in K/Al_2O_3 CO production corresponded to 60% of $^{13}CO_2$ used in the reaction, whereas the ^{13}CO only corresponded to 36%. $^{12}CO/^{12}CO_2$ ratio is shown in Fig. 10. In spent Al_2O_3, $K/Al_2O_3$and $V\text{-}K/Al_2O_3$ catalysts, all peaks of ^{12}CO and $^{12}CO_2$ were used. Firstly, by increasing temperature, the ^{12}CO formation increased, as expected according to thermodynamics (the higher the temperature the higher conversion of the more endothermic reaction, *i.e.* CO formation); secondly, CO and CO_2 formation can be affected by the population of oxidized species on coke, oxygen mobility in the catalyst, type of chemical species, and yet each step should be differently catalyzed. This complexity hinders the comparison between K/Al_2O_3 and $V\text{-}K/Al_2O_3$ in terms of $^{12}CO/^{12}CO_2$ ratio, since similar conversions were observed at different temperatures. However, the lower ^{12}CO formation in the latter catalyst can be associated to a higher population of oxidized species or higher oxygen migration in the catalyst, caused by the higher $^{13}CO_2$ conversion at lower temperatures, which as observed during carbon gasification largely favors $^{12}CO_2$ release. Finally, it is also important to mention that neither H_2O nor H_2 were simultaneously released with the above products, therefore we can rule out $^{12}CO_2$ formation by water gas shift reaction [52].

Table 4
RB reaction using $^{13}CO_2$[a] on $V\text{-}K/Al_2O_3$ and K/Al_2O_3 catalysts, conversion expressed in coke consumption.

Temperature (°C)	% of carbon in coke converted in spent $V\text{-}K/Al_2O_3$[b]	% of carbon in coke converted in spent K/Al_2O_3[b]
680	28	n.d.
720	46	11
760	67	23
800	89	48
860	n.d.	74

[a] Total of $^{13}CO_2$ introduced in the reactor was 0.472 mmol.
[b] Total carbon amount in coke, assuming that coke is solely composed by carbon, for $V\text{-}K/Al_2O_3$ and K/Al_2O_3 are 0.283 and 0.35 mmol, respectively.

4. Discussion

Coke gasification in the presence of O_2 and CO_2 has been pointed as a very complex reaction [14], problem that becomes more difficult on a catalyst surface. Still, from the above results, it is clear that these reactions are largely improved on the $V\text{-}K/Al_2O_3$ catalyst.

By means of XPS characterization, it was shown that potassium only covered a small portion of alumina surface. On the other hand, potassium mobility, which was reported to occur at high temperatures (700–800 °C) [19], could not take place during oxidation in O_2 atmosphere, as it takes place at smaller temperatures. Yet, coke mobility, as far as we know, has not been reported in the literature. O_2 and atomic oxygen mobility is a well known process and it is often associated to a decrease on coke burning temperatures [53]. The same idea could be extended to CO_2 activation. When both potassium and vanadium were put together coke burning temperatures were much reduced. According to these results it is possible to assert a synergy effect between vanadium and potassium that highly reduces the temperature at which the spillover oxygen is formed and becomes active. Since complete coke conversion is always achieved, it appears that O_2 and CO_2 are activated in a catalytic site near coke and then oxygen mobility derived by O_2 or CO_2 is taking place. However, potassium mobility cannot be ruled-out at higher temperature.

Concerning the catalytic sites of $V\text{-}K/Al_2O_3$ there are two main possibilities: O_2 and CO_2 could be activated in a catalytic site composed by both potassium and vanadium or, alternatively, a redox cycle could take place (as proposed for dehydrogenation reaction in CO_2 [54]). During RB reaction vanadium could undergo reduction (by reacting with coke) followed by oxidation of either CO_2 or O_2, however, oxygen mobility is necessary to occur on alumina.

Soft oxidant reactions of hydrocarbons on vanadium catalysts in the presence of O_2 and CO_2 are related to a vanadium redox cycle. The former is a class of reaction largely explored [55], including in the presence of potassium [56], the later has been explored more recently [13]. Two mechanisms were proposed: CO_2 can be decomposed on active sites to form CO and an active oxygen species, or alternatively, one oxygen atom transfer from CO_2 to vacant oxygen sites (saturated hydrocarbon is oxidized to unsaturated hydrocarbon while vanadium is reduced to lower oxidation state forming water). In fact, our group performed an experiment in which a previously reduced $V\text{-}K/Al_2O_3$ was put to react with labeled carbon $^{13}CO_2$ [40]. $^{13}CO_2$ was reduced to ^{13}CO while oxidizing the vanadium. However, when both $^{13}CO_2$ and O_2 were introduced, no ^{13}CO was observed [40]. These results were related

Equation 1-a $\mathbf{C}O_2 + *C \rightarrow \mathbf{C}O_2*C$

Equation 1-b $\mathbf{C}O_2 + VK_s*C \rightarrow VK_s\mathbf{C}O_2*C$

Equation 1-c $VK_s\mathbf{C}O_2*C \rightarrow \mathbf{C}O + VK_sO*C$

Equation 1-d $O_2 + VK_s*C \rightarrow VK_sO_2*C$

Equation 1-e $VK_sO_2*C + *C \rightarrow VK_sO*C + O*C$

Equation 1-f $VK_sO*C + *C \rightarrow VK_s*C + O*C$

Equation 1-g $VK_sO*C + O*C \rightarrow VK_sO*C + O_2*C$

Equation 2 $O*C + O*C \rightarrow O_2*C + *C$

Equation 3 $O_2*C \rightarrow CO_2$

Equation 4 $O_2*C + *C \rightarrow CO + O*C$

Equation 5 $O*C \rightarrow CO$

Equation 6 $\mathbf{C}O + *C \rightarrow \mathbf{C}O*C \rightarrow CO + *\mathbf{C}$

Scheme 2. Set of reaction step for both RB and O_2 reaction with coke on spent catalyst.

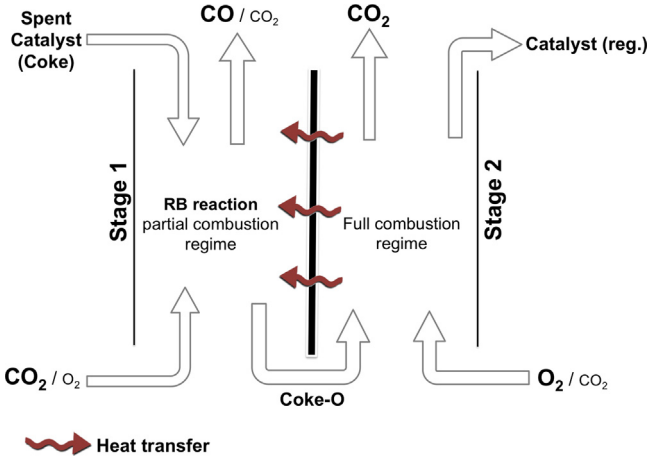

Fig. 11. Two stage FCC regeneration with diathermy wall provides heat transfer between the stages. Stage 1 favors RB reaction by work on high CO_2 and low O_2 partial pressure. The stage 2 works at high O_2 partial pressure in order to burn residual coke from stage 1 and provide heat for the overall FCC process.

to the faster oxidation activity of oxygen when compared to CO_2. Considering that this catalyst was remarkably active for RB reaction in the presence of oxygen, the catalyst sites that activate CO_2 and O_2 must be composed by both V and K atoms. The catalytic effect of potassium on glassy carbon surfaces was attributed to potassium–oxygen–coke compound formation [19]. Moreover, peroxocarbonate species over metal complexes were evidenced by spectroscopic studies [57]. Therefore, as vanadium and potassium are close in V-K/Al_2O_3, it could be possible that both potassium and vanadium participated in the RB reaction pathway, probably by forming more reactive carbonate species. This possibility could be coupled to higher oxygen mobility on potassium compared with pristine alumina. This possibility is supported by the reactivity of spent alumina catalysts in RB reaction that followed the order: K/Al_2O_3 > Mg/Al_2O_3, Li/Al_2O_3 > Ca/Al_2O_3, Na/Al_2O_3 > Al_2O_3 (based on the temperature range and the amount of CO produced in Fig. 5). This sequence did not follow any obvious property, as for example in soft oxidation, where CO_2 activity is correlated to charge/ratio ratio of alkaline metal [13].

Currently reaction steps involved in coke burn under O_2 atmosphere are proposed in Ref. [58], these steps are extended to CO_2 in Scheme 2. In the presence of a catalyst, step 1-a can be rule out. CO_2 activation is represented by step 1-b and ^{13}CO formation by step 1-c. O_2 activation comprises steps 1-d and 1-e. After either CO_2 or O_2 reaction with coke an oxidized group represented in Eqs. (1-c) and (1-e) undergoes oxygen mobility on the catalyst surface as represented by step 1-f. In addition, after reacting with coke, as already proposed at moderate oxygen coverage for glassy carbon surfaces [14], these oxidized groups were equivalent for both atmosphere. Sequentially to these steps ^{12}CO and $^{12}CO_2$ are formed according to the literature in steps 3–5 [21]. ^{12}CO would be favored when reaction temperature increases, as observed. Kelemen et al. [14] in a comprehensive work on glassy carbon surfaces showed that the energy barrier for CO release decreases when oxygen coverage on carbon increases, yet differences between CO_2 and O_2 were apparent at high oxygen coverage.

During RB reaction on pure CO_2 the $^{12}CO/^{12}CO_2$ ratio in the most active catalyst (V-K/Al_2O_3) was lower than in K/Al_2O_3. Therefore, the amount of O*C species on coke could attain a steady-state-conditions, these species could be related with active oxygen, as represented in Eq. (1-f), which produced high amounts of $^{12}CO_2$, as represented by Eq. (3). Finally, Eq. (6) was discarded based on ^{13}C NMR in spent catalyst after exposed to labeled carbon $^{13}CO_2$ and regular CO_2 [59].

4.1. Outlook

These findings support the proposition of performing the partial RB reaction (Scheme 1a) followed by sequential or simultaneous residual coke burning in the presence of oxygen as represented by Scheme 1c. This type of catalyst should be introduced separately, as an additive, or introduced in the main catalyst composition. Currently, FCC units could be retrofit in order to introduce and recycle CO_2. CO selectivity and heat balance could be achieved by a proper choice of O_2 partial pressure and the amount of additive (for RB reaction)/FCC catalyst. In longer terms two-stage FCC regeneration could be designed, as presented in Fig. 11, RB reaction would be favored in the first one using high CO_2 partial pressure and very low amount of O_2, residual coke would be burned in the second stage using high O_2 partial pressure providing energy to step one and to the overall FCC process.

5. Conclusions

FCC spent catalyst regeneration could be performed in CO_2 rich atmosphere. This approach can largely contribute to mitigate CO_2 emissions in the refinery and produce CO for sequential uses. Moreover, this reaction should be performed in the presence of O_2 in order to keep the process heat balance under regular FCC temperature, *i.e.* 700–720 °C. Alumina modified by groups I and II elements could be used for such propose, particularly when modified with potassium. Vanadium and potassium showed a synergism that largely favored the CO_2 and coke reaction.

$^{13}CO_2$ and coke reaction on the catalysts firstly released ^{13}CO, almost simultaneously followed by regular ^{12}CO and $^{12}CO_2$. These species were also formed dislocated to larger time-on-stream. Both the type of catalyst and reaction temperature largely affected the ^{12}CO and $^{12}CO_2$ species in RB reaction. Particularly, vanadium and potassium catalyst showed all species formed in one main region. Besides, this spent catalyst was also highly active to be regenerated in O_2/He atmosphere. The results suggest that coke burned by either CO_2 or O_2 is comprised by mainly two steps, activation of these species on V-K sites followed by oxygen mobility, which is affected by the type of the catalyst.

Acknowledgment

To CNPq, CAPES, PETROBRAS (under contract 4600250882) and FAPERJ for financial support.

Appendix A. Supplementary data

Supplementary data associated with this article can be found, in the online version, at http://dx.doi.org/10.1016/j.apcatb.2014.09.028.

References

[1] Key World Energy Statistics, International Energy Agency, 2012, pp. 80.
[2] X. Xiaoding, J.A. Moulijn, Energy Fuels 10 (1996) 305–325.
[3] O. Wild, The Straight Facts on Forests, Carbon, and Global Warming, 2007.
[4] M. Aresta, Carbon Dioxide Recovery and Utilization, Kluwer Academic Publishers, The Netherlands, 2003.
[5] P. O'Connor, Stud. Surf. Sci. Catal. 166 (2007) 227–251.
[6] M. Guisnet, F.R. Ribeiro, Deactivation and Regeneration of Zeolite Catalysts, Imperial College Press, London, 2011.
[7] J.R. Rostrup-Nielsen, L.J. Christiansen, J.H. Bak Hansen, Appl. Catal. 43 (1988) 287–303.
[8] G.C. Chinchen, P.J. Denny, D.G. Parker, M.S. Spencer, D.A. Whan, Appl. Catal. 30 (1987) 333–338.
[9] M. Stiefel, R. Ahmad, U. Arnold, M. Döring, Fuel Process. Technol. 92 (2011) 1466–1474.
[10] E.F. Sousa-Aguiar, L.G. Appel, C. Mota, Catal. Today 101 (2005) 3–7.
[11] A. Martinez, J. Rollan, M.A. Arribas, H.S. Cerqueira, A.F. Costa, E.F. S-Aguiar, J. Catal. 249 (2007) 162–173.
[12] D. Mark, Appl. Catal. A 189 (1999) 185–190.
[13] M.B. Ansari, S.-E. Park, Energy Environ. Sci. 5 (2012) 9419.
[14] S.R. Kelemen, H. Freund, Carbon 23 (1985) 723–729.
[15] J.F. Espinal, A. Montoya, F. Mondragon, T.N. Truong, J. Phys. Chem. B 108 (2004) 1003–1008.
[16] K.A. Essenhigh, Y.G. Utkin, C. Bernard, I.V. Adamovich, J.W. Rich, Chem. Phys. 330 (2006) 506–514.
[17] G.A. Olah, A. Goeppert, G.K.S. Prakash, J. Org. Chem. 74 (2009) 487–498.
[18] B. Marchon, W.T. Tysoe, J. Carrazza, H. Heinemann, G.A. Somorjai, J. Phys. Chem. 92 (1988) 5744–5749.
[19] S.R. Kelemen, H. Freund, J. Catal. 102 (1986) 80–91.
[20] M.M. Pereira, L. Benoit, in: S.L. Suib (Ed.), New and Future Developments in Catalysis: Catalysis for Remediation and Environmental Concerns, Elsevier, Amsterdam, 2013, pp. 535–562.
[21] C. Li, C. Le Minh, T.C. Brown, J. Catal. 178 (1998) 275–283.
[22] C. LeMinh, R.A. Jones, I.E. Craven, T.C. Brown, Energy Fuels 11 (1997) 463–469.
[23] S.R. Kelemen, D. Freude, Carbon 23 (1985) 619–625.
[24] M.B. Jensen, L.G.M. Pettersson, O. Swang, U. Olsbye, J. Phys. Chem. B 109 (2005) 16774–16781.
[25] K.B. Lee, A. Verdooren, H.S. Caram, S. Sircar, J. Colloid Interface Sci. 308 (2007) 30–39.
[26] F. Voigts, F. Bebensee, S. Dahle, K. Volgmann, W. Maus-Friedrichs, Surf. Sci. 603 (2009) 40–49.
[27] S. Walspurger, L. Boels, P.D. Cobden, G.D. Elzinga, W.G. Haije, R.W. van den Brink, ChemSusChem 1 (2008) 643–650.
[28] J.F. Munera, S. Irusta, L.M. Cornaglia, E.A. Lombardo, D.V. Cesar, M. Schmal, J. Catal. 245 (2007) 25–34.
[29] A. Nandini, K.K. Pant, S.C. Dhingra, Appl. Catal. A 308 (2006) 119–127.
[30] K. Nagaoka, K. Seshan, J.A. Lercher, K. Aika, Catal. Lett. 70 (2000) 109–116.
[31] R. Bouarab, O. Akdim, A. Auroux, O. Cherifi, C. Mirodatos, Appl. Catal. A 264 (2004) 161–168.
[32] S.R. Mirzabekova, G.T. Farkhadova, A.K. Mamedov, M.I. Rustamov, React. Kinet. Catal. Lett. 48 (1992) 225–231.
[33] Y.H. Cui, H.D. Zhang, H.Y. Xu, W.Z. Li, Appl. Catal. A: Gen. 318 (2007) 79–88.
[34] F. Solymosi, P. Tolmacsov, T.S. Zakar, J. Catal. 233 (2005) 51–59.
[35] T. Blasco, J.M.L. Nieto, Appl. Catal. A (1997) 117–142.
[36] C. Resini, M. Panizza, L. Arrighi, S. Sechi, G. Busca, R. Miglio, S. Rossini, Chem. Eng. J. 89 (2002) 75–87.
[37] A.S. Escobar, F.V. Pinto, H.S. Cerqueira, M.M. Pereira, Appl. Catal. A 315 (2006) 68–73.
[38] A. Escobar, M. Pereira, R. Pimenta, L. Lau, H. Cerqueira, Appl. Catal. A 286 (2005) 196–201.
[39] R.P. dos Santos, T.C. da Silva, M.L.A. Gonçalves, B. Louis, E.B. Pereira, M.H. Herbst, M.M. Pereira, Appl. Catal. A 449 (2012) 23–30.
[40] T.C. da Silva, R.P. dos Santos, N. Batalha, M.M. Pereira, Catal. Commun. 51 (2014) 42–45.
[41] L.T. dos Santos, F.M. Santos, R.S. Silva, T.S. Gomes, P.M. Esteves, R.D.M. Pimenta, S.M.C. Menezes, O.R. Chamberlain, Y.L. Lam, M.M. Pereira, Appl. Catal. A 336 (2008) 40–47.
[42] J. Scholz, A. Walter, T. Ressler, J. Catal. 309 (2014) 105–114.
[43] J. Liu, Z. Zhao, C. Xu, A. Duan, L. Zhu, X. Wang, Catal. Today 118 (2006) 315–322.
[44] H. García, J. López Nieto, E. Palomares, B. Solsona, Catal. Lett. 69 (2000) 217–221.
[45] M.C. Manchado, J.M. Guil, A.P. Masia, A.R. Paniego, J.M.T. Menayo, Langmuir 10 (1994) 685–691.
[46] M. Almarri, X.L. Ma, C.S. Song, Energy Fuels 23 (2009) 3940–3947.
[47] L.T.d. Santos, F.M. Santos, R.S. Silva, T.S. Gomes, P.M. Esteves, R.D.M. Pimenta, S.M.C. Menezes, O.R. Chamberlain, Y.L. Lam, M.M. Pereira, Appl. Catal. A 336 (2008) 40–47.
[48] Z. Zhang, Y. Zhang, Z. Wang, X. Gao, J. Catal. 271 (2010) 12–21.
[49] L. Castoldi, R. Matarrese, L. Lietti, P. Forzatti, Appl. Catal. B 90 (2009) 278–285.
[50] Y. Wu, J. Wang, S. Wu, S. Huang, J. Gao, Fuel Process. Technol. 92 (2011) 523–530.
[51] D.M. Stockwell, Test methods for simulating fcc regenerator catalysis and catalyst deactivation, US 20070166826 A1 (2007).
[52] C. Ratnasamy, J.P. Wagner, Catal. Rev. Sci. Eng. 51 (2009) 325–440.
[53] B.K. Vu, E.W. Shin, Catal. Lett. 141 (2010) 699–704.
[54] K. Saito, K. Okuda, N.O. Ikenaga, T. Miyake, T. Suzuki, J. Phys. Chem. A 114 (2010) 3845–3854.
[55] X. Rozanska, R. Fortrie, J. Sauer, J. Phys. Chem. C 111 (2007) 6041–6050.
[56] G. Garcia Cortez, J.L.G. Fierro, M.A. Bañares, Catal. Today 78 (2003) 219–228.
[57] M. Aresta, I. Tommasi, E. Quaranta, C. Fragale, J. Mascetti, M. Tranquille, F. Galan, M. Fouassier, Inorg. Chem. 35 (1996) 4254–4260.
[58] C. Li, T.C. Brown, Energy Fuels 13 (1999) 888–894.
[59] A.P.S.S. Estevão, F.M. Santos, M.L.A. Gonçalves, R.A. San Gil, H.S. cerqueira, B. Louis, M.M. Pereira, Adv. Chem. Lett. 1 (2013) 1–9.